FRIGID ZONE **MEDICINE**
Original Article • DOI: 10.2478/fzm-2023-0015

Cold exposure alters proteomic profiles of the hypothalamus and pituitary in female rats

Xiangyu Bian[#], Xi Li[#], Tong Xu, Li Zhang, Yongqiang Zhang, Shuai Wu, Renren Yang, Weiyun Dong, Changjiang Guo, Danfeng Yang[*], Weina Gao[*]

Abstract

Objective: Studies have shown that both short-term and long-term cold exposures disturb the biological process. The aim of the present study is to investigate the effects of intermittent cold exposure on proteomic profiles in the hypothalamus and pituitary of female Sprague-Dawley (SD) rats. **Materials and methods:** The rats were exposed to -10°C in a cabin for 4 h per day, and the treatment lasted for 14 days. The comparative label-free LC-MS/MS analysis was performed to investigate the changes of proteomic profiles in the hypothalamus and pituitary. ELISA analysis was used to validate the expression of differential proteins. **Results:** 22 differential proteins in the hypothalamus and 75 differential proteins in the pituitary were identified by the label-free proteomic analysis. Gene ontology annotation and enrichment analysis indicated that cold exposure disrupted protein phosphorylation, filopodium assembly, intracellular protein transport, peripheral nervous system neuron axonogenesis, spinal cord development, Golgi organization, positive regulation of pseudopodium assembly, and cell-cell adhesion. Three proteins (Cdc42, Ptprs, and Setd7) were down-regulated in the cold exposure group. **Conclusion:** The results indicate that intermittent cold exposure alters the proteomic profiles of hypothalamus and pituitary in female rats.

Keywords

cold exposure; proteomic profile; hypothalamus; pituitary

Received 10 November 2021, accept 20 September 2022

Tianjin Institute of Environmental and Operational Medicine, Tianjin 300050, China

**Corresponding author Danfeng Yang, E-mail: fengdyd@126.com; Weina Gao, E-mail: gwn2004bo@126.com*
[#]These authors contributed equally to this work

1 Introduction

The reception of cold stress signals is controlled by the hypothalamus. Previous studies have shown that cold exposure induces alteration of biological process and changes of protein expression. Acute cold exposure (-10°C for 2 h) causes disruption of the biological process including catecholamines, glucocorticoids, gut microbiota and tryptophan metabolism, and the tricarboxylic acid (TCA) cycle[1]. After a short-term cold exposure (4 ± 1)°C for 24 h, the rates of protein synthesis is decreased, while the Ca^{2+}-dependent proteolytic processes is increased in skeletal muscles[2]. After exposure to 7-8°C cold environment for 48 h, the balance between oxidants and antioxidantsin rats was broken and the hypothalamic–pituitary–adrenal axis was impaired[3]. After exposure to 4°C for longer than 7 days, the activity of adenosine 5'-monophosphate-activated protein kinase (AMPK) in brown or white adipose tissue of mice is enhanced and the expression of AMPK-1α in brown adipose tissue was up-regulated[4]. Long-term cold exposure (immersed in shoulder-deep water of approximately 18°C for 1 h/d, 5 d/week, for 20 weeks) results in a shift of the contractile properties of fast-twitch muscle toward the slow-twitch type[5].

Maintaining the core body temperature in a cold environment is important for the survival of homeotherms. Body temperature is controlled by the thermoregulatory center of hypothalamus[6]. Cold-induced thermogenesis includes shivering thermogenesis and non-shivering thermogenesis in muscle and brown adipose tissue, respectively. A study suggested that the hypothalamus controls brown adipose tissue thermogenesis[7]. Brown adipose tissue content was related to the level of cold-induced thermogenesis[8]. Uncoupling protein 1 in brown adipose tissue mediates the heat release in rodents[9]. Cold exposure induces release of thyrotropin-releasing hormone in the paraventricular nucleus and thyrotropin in the anterior-pituitary[10]. These hormones act as regulators to increase thermogenesis in brown adipose tissue. Despite that cold exposure interfering with

various metabolic processes in the hypothalamus and pituitary has been implicated by many studies, the mechanisms of these abnormalities have not yet been well elucidated so far.

In this study, the female rats were exposed to -10°C in a cabin for 4 h/day for consecutive 14 days. The comparative label-free LC-MS/MS analysis was performed to explore the differential expressed proteins (DEP) in the hypothalamus and pituitary. The aim of the present study was to characterize the changes of proteomic profiles and explore the molecular mechanisms underlying the effects of cold exposure.

2 Materials and methods

2.1 Animal treatments

Animal handling and treatment were approved by the Animal Ethical Committee of the Department of Scientific Management of Tianjin Institute of Environmental and Operational Medicine (IACUC of AMMS-04-2020-017). Twenty female Sprague-Dawley (SD) rats (210-230 g), purchased from Beijing Vital River Laboratory Animal Technology Co., Ltd., were housed in cages. The ambient temperature was controlled at between 22°C and 25°C and relative humidity between 40% and 60%, with 12 h light/dark cycles.

After being acclimatized on rodent chow for 7 days, the rats were randomly divided into the control (C) group and the cold exposure (CE) group, with 10 rats in each group. The rats of the CE group were exposed to -10°C in a cabin for 4 h per day, and were treated for 14 days. During cold exposure, each rat was housed in a separate cage to avoid mutual contact for warmth. The rats of the control group were feed at 22-25°C. After 14 days, the female rats were sacrificed for the collection of samples. Hypothalamus and pituitary tissues were immediately rinsed and cleaned with ice-cold saline and frozen in liquid nitrogen until use.

2.2 Label-free Quantification (LFQ) proteome analysis

2.2.1 Sample preparation

Total protein samples were extracted and concentrated in 5 mmol/L tris (2-carboxyethyl) phosphine on the 55°C water bath for 10 min, and then alkylated with 10 mmol/L iodoacetamide in the room temperature for 15 min. The samples were digested with 0.05 μg/μL trypsin solution at 37°C overnight. The peptides were desalted on C18 columns (3M Bioanalytical Technologies), freeze-dried by vacuum and reconstituted in 0.1% (V/V) formic acid and 2% acetonitrile (1 μg/μL).

2.2.2 Nano-ultro phase liquid chromatography-Q exactive for protein analysis

Chromatographic separation of peptide mixture was carried out on a nano-UPLC device (EASY-nLC1200, Thermo Scientific, USA) coupled with a C18 reversed-phase analytical column (Reprosil-Pur 120 C18-AQ, 1.9 μm, 15 cm long, 100 μm inner diameter, Thermo Scientific, USA) in buffer A (0.1% formic acid and 2% acetonitrile) and separated with a linear gradient of buffer B (0.1% formic acid and 80% acetonitrile) at a flow rate of 0.3 μL/min controlled by IntelliFlow technology. The gradient varied from 8%-35% in solvent B for 92 min to 35%-45% for 20 min, 45%-100% for 2 min and 100% for another 2 min. Finally, the gradient was changed from 100%-2% in solvent B for 2 min to 2% solvent B for another 2 min. Spectrascans were acquired in Q-Exactive™ mass spectrometry instrument (Thermo Scientific, USA).

Mass spectrum (MS) data were acquired using a data-dependent top20 method dynamically to choose the most abundant precursor ions from the survey scan (350-1 600 m/z) for HCD fragmentation. Automatic gain control (AGC) was enabled, and MS1 targets were set to 3×10^6 and MS2 targets were set to 1×10^5. Maximum inject time (Max IT) was 50 ms for MS1 and 45 ms for MS2. Normalized collision energy (NCE) was set at 28% and the dynamic exclusion of 40 s. Data were collected in positive mode with an MS1 resolution of 70 000 and an MS2 resolution of 17 500 at m/z 200.

2.2.3 Bioinformatic analyses

The MS data were analyzed using MaxQuant software (version 1.5.6.0.) (Max Planck Institute of Biochemistry, Germany) based on the Uniprot-RAT-2016-09 databases. The DEP were analyzed using the search tool DAVID (http://david.abcc.ncifcrf.gov) for GO annotation and enrichment analysis, which includes three main modules: biological process (BP), cellular component (CC) and molecular function (MF). The web-based Kyoto Encyclopedia of Genes and Genomes (KEGG, http://www.genome.p/kegg) was used for pathway analysis (Kanehisa *et al.*, 2012). STRING (http://string.embl.de) was used as a database for predicting signaling networks and protein interactions (Deng *et al.*, 2015). Hierarchical cluster was performed using Blast2GO (Version 3.5.0). Fold > 1.5, $P < 0.05$, and unique peptide ≥ 2 was defined as DEP.

2.3 Enzyme-linked immunosorbent assay (ELISA) validation of differentially expressed proteins from LFQ

To quantitatively validate the results of the LFQ proteomic analysis, the protein expression levels of Cdc42, Mfn2, and Ptprs in the hypothalamus and Ctbp2, Cdc42, Setd7, Tom1 and activity

of Setd7 in the pituitary were further determined by the ELISA method. The ELISA kits were purchased from Jianglai Biological Technology Company Limited (Shanghai, China). The results were normalized by protein content determined by bicinchoninic acid (BCA) assay.

2.4 Statistical analysis

Data are presented as mean value and standard deviation (N = 10) and were analyzed by t-test using SPSS 20.0 (SPSSInc., Chicago, IL, USA). Statistical significance was considered when $P < 0.05$.

3 Results

3.1 Changes of proteomic profiles after cold exposure

Proteome analysis identified 3 346 proteins in the hypothalamus and 3352 proteins in the pituitary (Fold > 1.5, $P < 0.05$, and false discovery rate (FDR) < 0.01). Compared with the C group, 22 proteins significantly changed in the hypothalamus (Fold > 1.5, $P < 0.05$) with 9 up-regulated and 13 down-regulated with a magnitude of fold change ranging from 0.21 to 14.26 (Table 1). 75 proteins significantly changed in the pituitary (Fold > 1.5, $P < 0.05$) with 50 up-regulated and 25 down-regulated with a magnitude of fold change ranging from 0.03 to 7.34 (Table 2). In the hypothalamus, the top 5 up-regulated proteins were Slc1a3, Cdk9, Sncb, Nudt9, and Gnpda1, and the top 5 down-regulated proteins were Mfn2, Atp6v1f, Mylk, Prkaa1, and Cdc42 (Table 1). In the pituitary, the top 5 up-regulated proteins were Prph, ATP6, Lage3, Clcn6, and Nefh, and the top 5 down-regulated proteins were Mycn, Edf1, Rbbp9, Tom1, and Arfgap3 (Table 2). The DEP between the C and CE groups was displayed by Volcano plot (Fig. 1) and heatmap as well. Clustering analysis showed that Cdc42 was differentially expressed in the hypothalamus and pituitary (Fig. 2).

3.2 GO annotation and pathway analysis

GO annotation showed that the DEP in the hypothalamus was significantly involved in biological processes with 18.8% being associated with protein phosphorylation and 9.0% with filopodium assembly (Fig. 3A). The biological processes significantly enriched in the pituitary included intracellular protein transport (7.0% association), peripheral nervous system neuron

Table 1 Differentially expressed proteins in hypothalamus

Entrez ID	Protein name	Protein description	Fold change	*P*-value
100911485	Mfn2	Mitofusin 2; Mitofusin 2, isoform CRA_a	0.21	0.001 1
116664	Atp6v1f	V-type proton ATPase subunit F	0.22	0.006 4
288057	Mylk	myosin light chain kinase, smooth muscle	0.30	0.001 0
65248	Prkaa1	5'-AMP-activated protein kinase catalytic subunit alpha-1	0.42	0.007 8
64465	Cdc42	Cell division control protein 42 homolog	0.48	0.002 8
25529	Ptprs	protein tyrosine phosphatase, receptor type, S	0.55	0.007 2
25600	Utrn	utrophin	0.56	0.005 9
293017	Bclaf1	BCL2-associated transcription factor 1	0.57	0.004 5
54238	Cdkn2c	cyclin-dependent kinase 4 inhibitor C	0.62	0.003 7
29483	Slc1a3	Excitatory amino acid transporter 1	1.68	0.014 7
362110	Cdk9	Cyclin-dependent kinase 9	1.72	0.007 9
113893	Sncb	Beta-synuclein	2.09	0.000 2
305149	Nudt9	ADP-ribose pyrophosphatase, mitochondrial	2.20	0.014 0
683570	Gnpda1	glucosamine-6-phosphate deaminase 1	2.30	0.009 4
690599	Mxra7	matrix-remodelling associated 7	2.45	0.003 7
79115	Evl	ena/VASP-like protein	2.97	0.003 0
84686	Ppp1r9b	Neurabin-2	3.23	0.002 7
362630	Srsf10	serine/arginine-rich splicing factor 10	3.56	0.001 1
25417	Dpysl4	Dihydropyrimidinase-related protein 4	3.68	0.014 0
116697	Pabpn1	polyadenylate-binding protein 2	5.76	0.002 1
304805	Cyb5r1	NADH-cytochrome b5 reductase 1	6.58	0.000 4
361732	Tmem109	Transmembrane protein 109	14.26	0.012 1

Table 2 Differentially expressed proteins in pituitary

Entrez ID	Protein name	Protein description	Fold change	*P*-value
298894	Mycn	N-myc proto-oncogene protein	0.03	0.000 2
296570	Edf1	Endothelial differentiation-related factor 1	0.09	0.000 7
29459	Rbbp9	Putative hydrolase RBBP9	0.16	0.021 7
361370	Tom1	target of Myb protein 1	0.16	0.033 9
503165	Arfgap3	ADP-ribosylation factor GTPase-activating protein 3	0.23	0.002 5
296284	Kif3b	kinesin-like protein KIF3B	0.27	0.030 9
307474	Tcerg1	transcription elongation regulator 1	0.28	0.007 2
305851	Supt16h	FACT complex subunit SPT16	0.28	0.003 6
50688	Cacnb1	voltage-dependent L-type calcium channel subunit beta-1	0.28	0.004 9
297568	A1i3	alpha-1-inhibitor 3 precursor	0.29	0.007 6
311880	Gapvd1	GTPase activating protein and VPS9 domains 1	0.29	0.005 8
688905	Mtx3	metaxin 3	0.32	0.022 6
360658	Gga3	ADP-ribosylation factor-binding protein GGA3	0.33	0.017 3
361796	Abhd16a	Abhydrolase domain-containing protein 16A	0.33	0.024 2
310652	Tdrkh	tudor and KH domain containing	0.33	0.012 7
361255	Tbce	Tubulin-specific chaperone E	0.34	0.003 5
25081	Apoa1	Apolipoprotein A-I	0.36	0.016 7
361925	Actl6a	actin-like protein 6A	0.37	0.009 4
259221	Osbpl1a	oxysterol-binding protein-related protein 1	0.38	0.005 9
302500	Mcts1	Malignant T-cell-amplified sequence 1	0.38	0.034 7
306204	Flnb	filamin-B	0.38	0.031 2
140594	Sytl4	synaptotagmin-like protein 4	0.40	0.012 7
289233	Pex19	peroxisomal biogenesis factor 19 isoform 1	0.42	0.046 0
294207	Ppp1r11	Protein phosphatase 1 regulatory subunit 11	0.42	0.039 8
64465	Cdc42	Cell division control protein 42 homolog	0.43	0.041 1
295284	Rbm8a	RNA-binding protein 8A	0.44	0.049 6
50592	Gria1	glutamate receptor, ionotropic, AMPA1 (alpha 1)	0.45	0.034 3
54301	Slc14a1	Urea transporter 1	0.46	0.006 4
312709	Mlf2	myeloid leukemia factor 2	0.46	0.027 5
108348048	Vwa5a	von Willebrand factor A domain containing 5A	0.47	0.042 3
297498	Crbn	Protein cereblon	0.48	0.013 5
288704	RGD1311899	Uncharacterized protein C12orf43 homolog	0.48	0.042 6
103690013	Nhp2	NHP2 ribonucleoprotein homolog	0.50	0.002 5
288064	Kpna1	importin subunit alpha-1	0.50	0.002 4
65165	Tmed2	Transmembrane emp24 domain-containing protein 2	0.50	0.001 9
171439	Bzw2	Basic leucine zipper and W2 domain-containing protein 2	0.52	0.016 4
25403	Cast	Calpastatin	0.54	0.014 9
171410	Acsbg1	Long-chain-fatty-acid--CoA ligase ACSBG1	0.54	0.000 5
291709	Slc25a46	Solute carrier family 25 member 46	0.55	0.020 3
140667	ENSRNOG00000018650	AP-3 complex subunit mu-2	0.58	0.022 9

Continued

Table 2 Continued

Entrez ID	Protein name	Protein description	Fold change	*P*-value
296099	Trp53bp1	transformation related protein 53 binding protein 1	0.59	0.039 7
502749	Agk	acylglycerol kinase, mitochondrial	0.60	0.016 9
680991	Tubg2	tubulin gamma-2 chain	0.60	0.035 4
171341	Mgst1	Microsomal glutathione S-transferase 1	0.62	0.033 5
306460	Enpp6	Ectonucleotidepyrophosphatase/phosphodiesterase family member 6	0.63	0.004 3
689954	Setd7	histone-lysine N-methyltransferase SETD7	0.65	0.009 1
100910616	Hmgn5	High mobility group nucleosome-binding domain-containing protein 5	0.65	0.028 5
29637	Hmgcs1	Hydroxymethylglutaryl-CoA synthase, cytoplasmic	0.65	0.003 5
293864	Ubl4a	Ubiquitin-like protein 4A	0.66	0.019 6
50872	Hpcal4	Hippocalcin-like protein 4	0.66	0.011 6
24688	Prph	peripherin	1.50	0.028 0
26197	ATP6	ATP synthase F0 subunit 6 (mitochondrion)	1.56	0.008 1
293863	Lage3	L antigen family member 3	1.62	0.032 9
295586	Clcn6	chloride transport protein 6	1.62	0.014 6
24587	Nefh	neurofilament heavy polypeptide	1.64	0.001 0
113960	Cdc42bpb	Serine/threonine-protein kinase MRCK beta	1.64	0.011 8
303653	Cdc42ep4	CDC42 effector protein (Rho GTPase binding) 4	1.65	0.034 6
289934	Oxsm	3-oxoacyl-ACP synthase	1.74	0.027 3
298757	Atl2	ADP-ribosylation factor-like 6 interacting protein 2	1.77	0.028 5
290651	Isyna1	Inositol-3-phosphate synthase 1	1.81	0.048 8
100361269	Snrpa1	small nuclear ribonucleoprotein polypeptide A'	1.88	0.043 4
311844	Ccbl1	kynurenine--oxoglutarate transaminase 1, mitochondrial	1.92	0.025 6
252892	Lgi1	Leucine-rich glioma-inactivated protein 1	2.13	0.000 6
81717	Ctbp2	C-terminal-binding protein 2	2.23	0.010 7
363465	Pir	Pirin	2.23	0.041 6
108350501	Rps29	40S ribosomal protein S29	2.45	0.043 7
66028	Arl6ip5	PRA1 family protein 3	2.53	0.041 3
300968	Uba5	Ubiquitin-like modifier-activating enzyme 5	2.76	0.039 9
25624	Vamp1	Vesicle-associated membrane protein 1	3.06	0.036 8
361288	Fundc2	FUN14 domain-containing protein 2	3.54	0.005 2
366602	Tspan13	Tetraspanin-13	3.94	0.004 4
64511	Fntb	Protein farnesyltransferase subunit beta	4.13	0.001 8
362093	Wdr5	WD repeat-containing protein 5	4.32	0.021 6
294421	Serinc1	Serine incorporator 1	5.00	0.001 2
84403	Gjb6	gap junction beta-6 protein	7.34	0.013 6

axonogenesis (2.8%), ovarian follicle atresia (2.8%), spinal cord development (4.2%), Golgi organization (4.2%), positive regulation of pseudopodium assembly (2.8%), and cell-cell adhesion (5.6%) (Fig. 3B).

GO annotation showed that the cellular components significantly involved in the hypothalamus are mainly associated with filopodium, neuronal cell body, extracellular exosome, growth cone, lamellipodium, nucleoplasm, synapse, cytoplasm, and cortical actin cytoskeleton. The cellular components significantly enriched in the pituitary are primarily localized in the cytoplasm, mitochondrial outer membrane, cytosol, nucleus, and neurofilament. In addition, the molecular function of these proteins in the hypothalamus is mainly associated with protein kinase

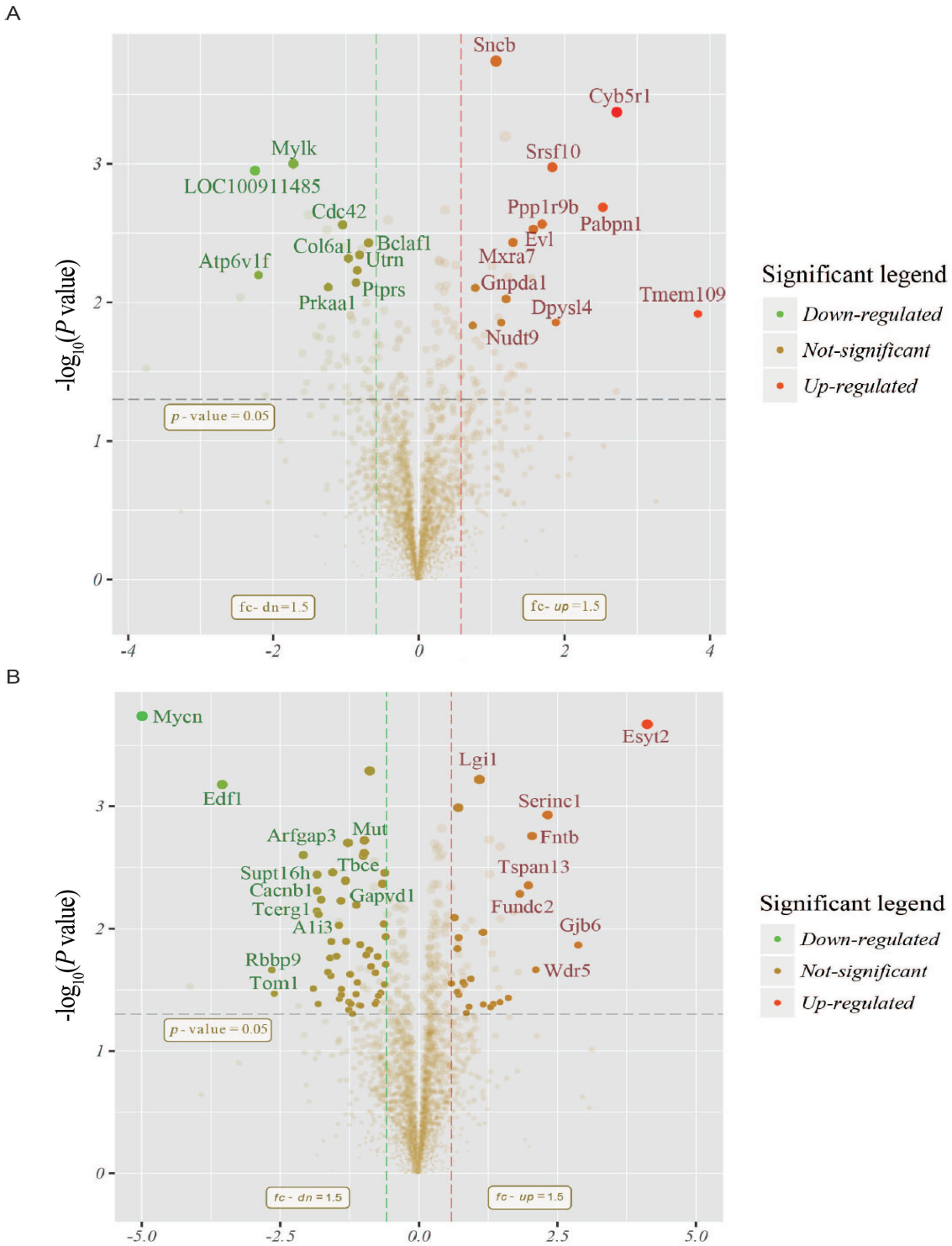

Fig. 1 Volcano plot depicting the proteomic alterations in the hypothalamus (A) and pituitary (B)

The red/green colors indicate points-of-interest that display both large magnitude fold-changes (x axis) and high statistical significance (-$\log_{10}$ of *P* value, y axis). The dashed horizontal line shows the *p*-value cutoff, and the two vertical dashed lines indicate down-/up-regulated proteins. Transparent points in the significant region means these proteins do not satisfy some other conditions.

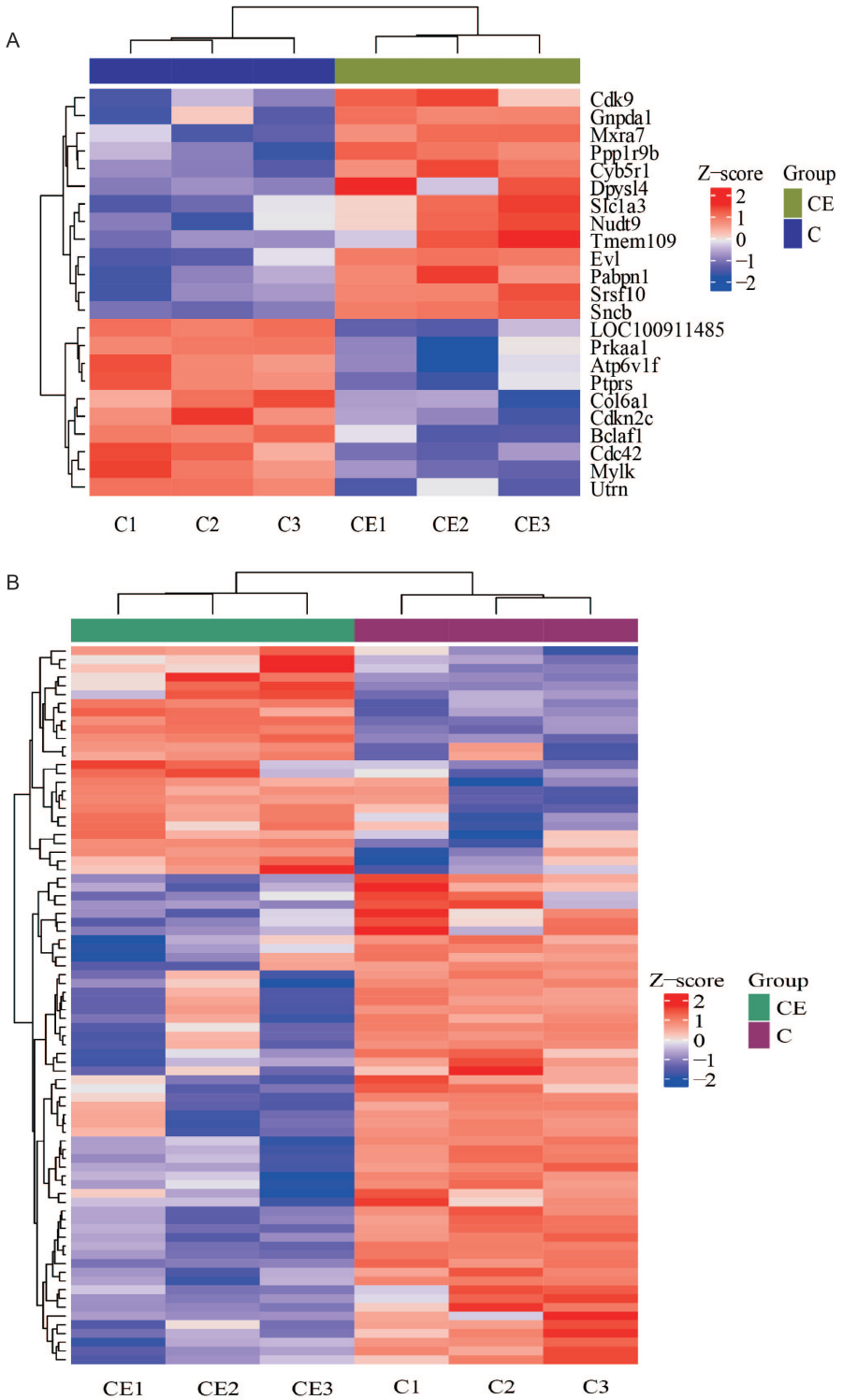

Fig. 2 Clustering heatmap of the significantly altered proteins in the hypothalamus (A) and pituitary (B) with an *FDR* < 1% identified by MaxQuant

Red, high expression; blue, low expression. Two main clusters of proteins can be observed, one up-regulated (right) and the other down-regulated (left) in the experimental group. Pearson's distance was used if the sample number equaled to or exceeded 3; otherwiseEuclidean's distance was used. C, control group; CE, cold exposure group.

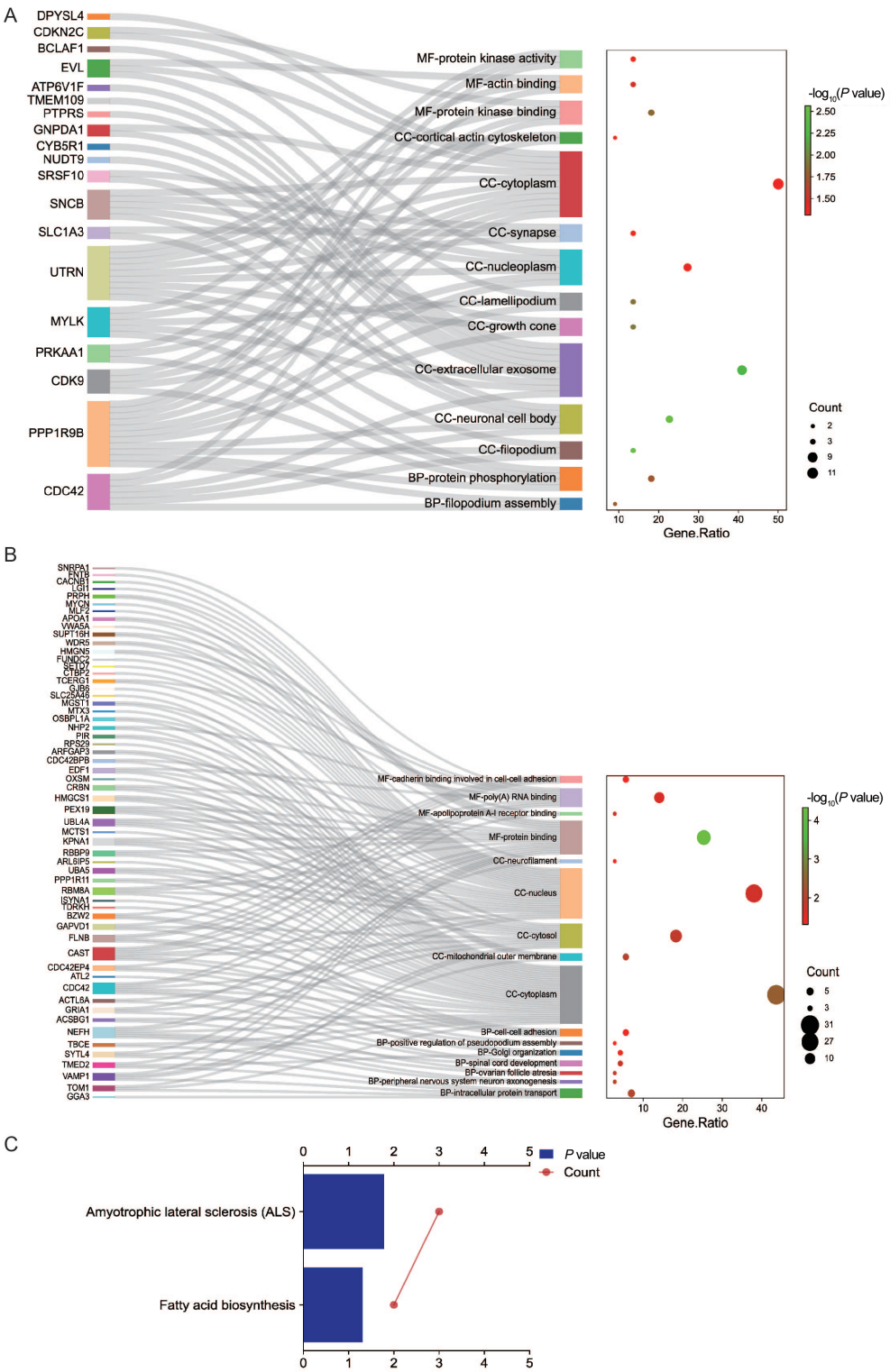

Fig. 3 Enriched GO iterms in the hypothalamus (A) and pituitary (B). Enriched KEGG pathways of the differentially expressed proteins in the pituitary (C)
The number of differentially expressed proteins was shown in the classification of biological process (BP), molecular function (MF) and cellular component (CC). The number of the altered proteins was shown in each KEGG pathway. The *P* value indicates the degree of enrichment.

binding, actin binding, and protein kinase activity. The molecular functions of the proteins significantly enriched in the pituitary mainly include in the protein binding, apolipoprotein A-I receptor binding, poly(A) RNA binding, and cadherin binding involving cell-cell adhesion.

The pathway analysis by KEGG on DEP predicted that the significantly affected pathways in the pituitary were amyotrophic lateral sclerosis (ALS) (down-regulate) and fatty acid biosynthesis (up-regulate) (Fig. 3C). No KEGG pathway was significantly enriched in the hypothalamus.

3.3 Protein interaction network analysis

Protein-protein interaction (PPI) network was analyzed using STRING and visualized with Cytoscape. As shown in Fig. 4, the PPI web consists of an intricately interconnected network with several DEP present at key hubs, and some of them function in a variety of biological processes. The most abundant subnetwork is involved in protein binding mediated by Ubl4a, which interacts with 25 proteins. Cdc42 is associated with 16 proteins and is involved in filopodium assembly and protein phosphorylation. Another protein with extensive connections is Tom1, which can interact with Ubl4aand Cdc42 and may play a critical role in the intracellular protein transport process.

3.4 ELISA validation of the differential expressed proteins

The protein expression levels of Cdc42, Mfn2, and Ptprs in the hypothalamus were further analyzed by ELISA. The results showed that the expressions of Cdc42 and Ptprs were significantly reduced in the CE group (Fig. 5). The protein expression levels of Ctbp2, Cdc42, Setd7 and Tom1 and activity of Setd7 in the pituitary were analyzed. The results showed that the activity of Setd7 was significantly reduced in the CE group (Fig. 5). This is consistent with the data obtained from the proteomic analysis.

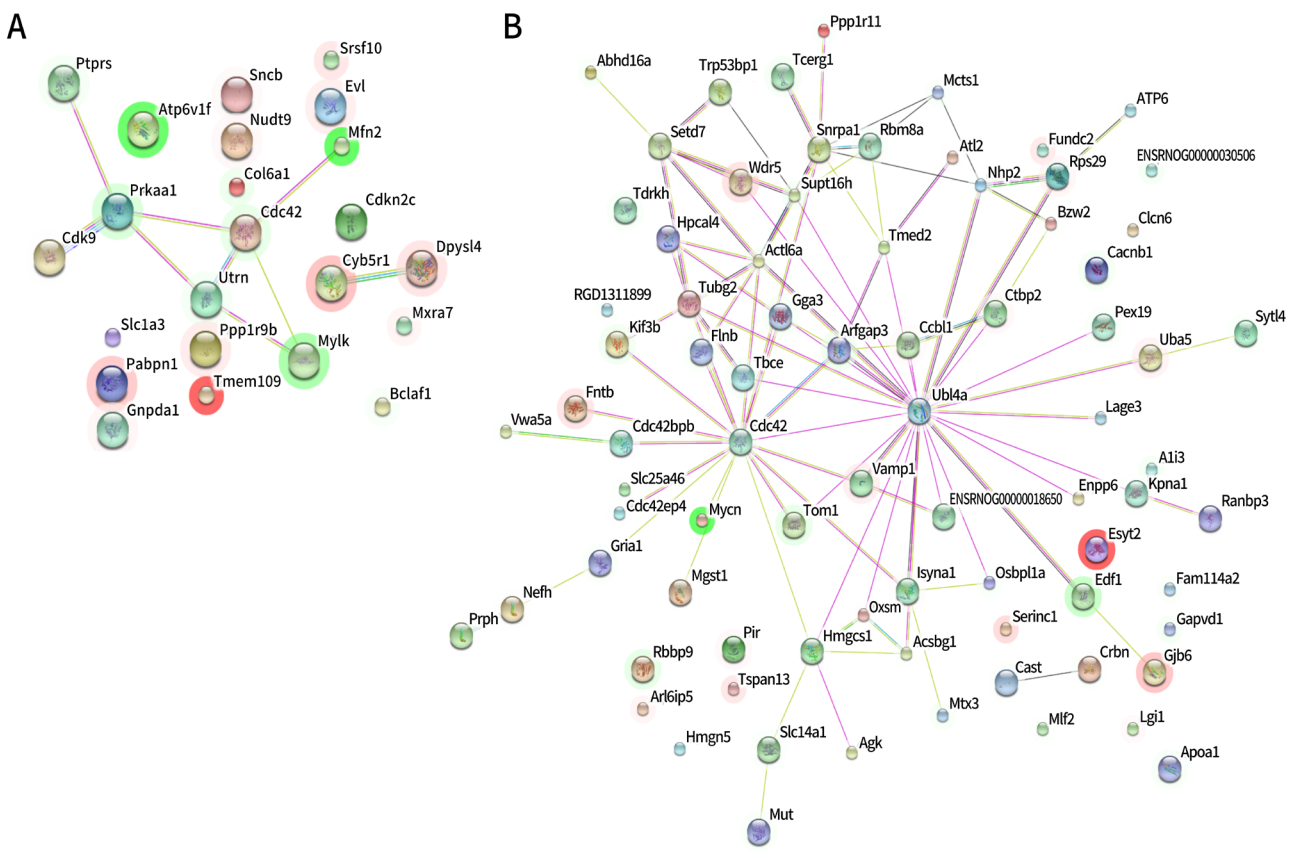

Fig. 4 STRINGdb protein-protein network enrichment analysis in the hypothalamus (A) and pituitary (B)
Different proteins are represented by nodes of different colors, with straight lines representing protein interactions, dark green and pink for currently known protein interactions, red, blue and green for expected interactions, and light blue, black and light green for other protein interactions.

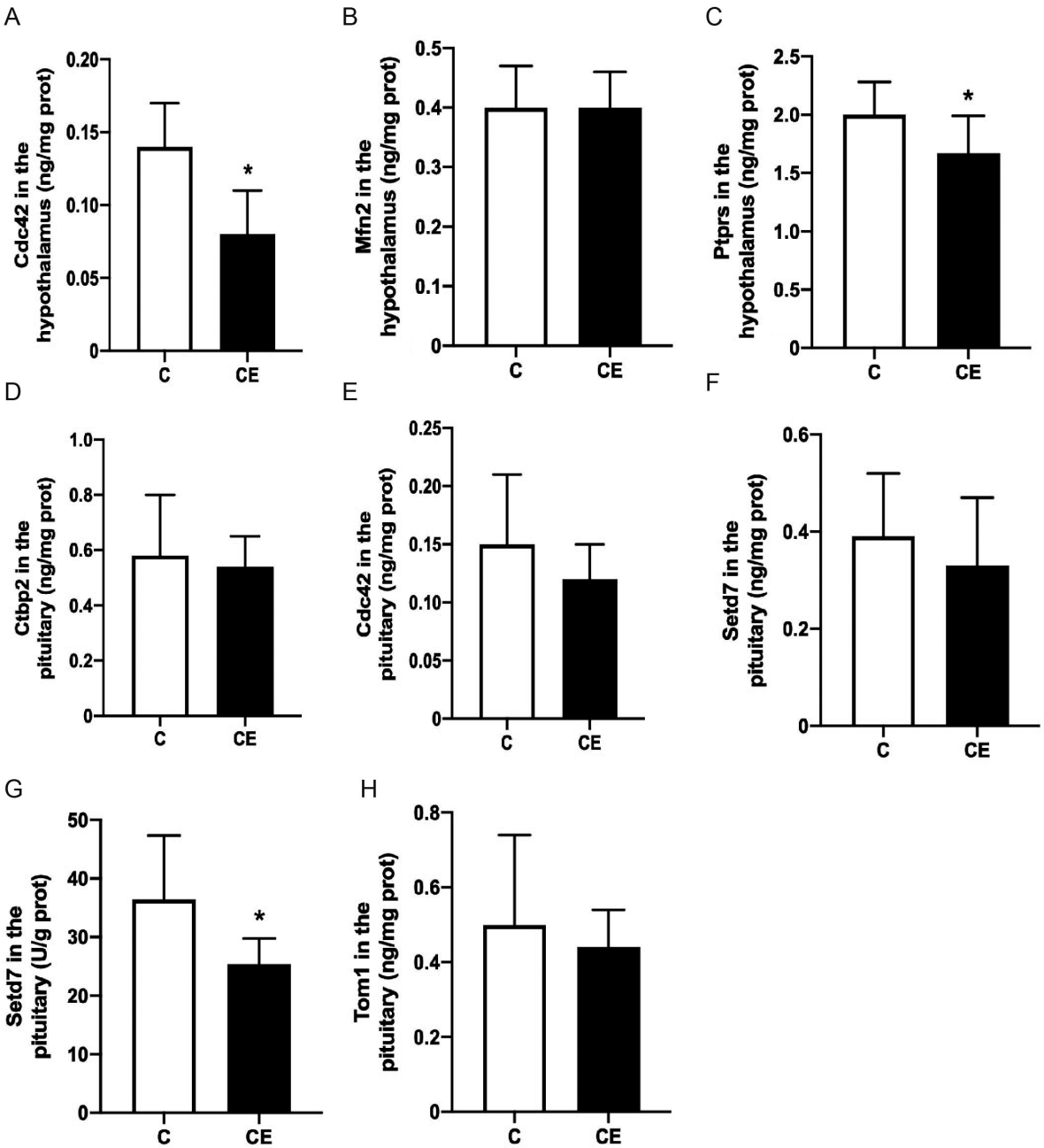

Fig. 5 ELISA analysis of the altered proteins induced by cold exposure in association with the enriched GO terms and KEGG pathways

Data are presented as mean values ± SD of protein levels. Results were normalized by total protein. $^{*}P < 0.05$ compared to the control group. C, control group; CE, cold exposure group.

4 Discussion

The expression of important protein markers, as well as the activities of certain enzymes was significantly changed after cold exposure. In the present study, intermittent cold exposure significantly altered the proteomic profiles in the hypothalamus and pituitary. Twenty-two proteins in the hypothalamus and 75 in the pituitary exhibited more than 1.5-fold changesin their expression levels.

Cdc42, Mfn2, and Ptprs were identified in the hypothalamus. GO analysis showed that Cdc42 is involved in filopodium

assembly process, Golgi organization, and positive regulation of pseudopodium assembly. Cdc42 is a GTPase of the Rho family regulating actin cytoskeletal remodeling in response to environmental signals. Cdc42 modulates multiple biological pathways involving filopodia formation, cell polarity, membrane retraction, migration, endocytosis, and cell cycle progression[11]. The GO analysis in this study also showed that filopodium assembly and positive regulation of pseudopodium assembly are linked to cold exposure. Filopodia acts as sensors of neurons and regulates ion channels to achieve signal transduction in adult animals[12]. Hence, Cdc42 may participate in the transmission of extracellular signals. A study demonstrated that p38 MAPK can be activated by Cdc42[13]. p38 MAPK, a stress-activated kinase that is involved in controlling physiological stress and neurological disorders, is important in regulating white adipose tissue thermogenesis[14]. In the present study, the expression of Cdc42 protein was significantly reduced in the hypothalamus. These data indicated that downregulation of Cdc42 may account for the thermogenic imbalance in response to cold exposure. Mfn2 is associated with cell cycle arrest and autophagy. Previous study demonstrated that Mfn2 repression impairs autophagy in mitochondria, leading to aggravation of mitochondrial dysfunction and apoptotic cell death in rat nucleus pulposus cells[15]. Ptprs is one of the proteins of the tyrosine phosphatase (PTP) family. PTPs are known to be signaling molecules that regulate a variety of cellular processes including dephosphorylation, cell growth, differentiation, mitotic cycle, and oncogenic transformation. Ptprs can suppress the signaling cascades that lead to the activation of Akt and MAPK[16]. Akt activation maintains cellular ATP content during acute cold exposure (-15°C for 4 h)[17]. In the present study, Ptprs was a component of exosomes enriched in the development process of cerebral cortex. Other studies have also reported similar results[18-19]. Proteomic analysis and ELISA revealed that the expression of Ptprs was significantly decreased in the hypothalamus of the CE group. It is possible that decrease in Ptprs promotes the acute energy production with intermittent cold exposure.

Cdc42, Tom1, Vamp1, Tmed2, Sytl4, Ctbp2, and Setd7 were found expressed in the pituitary. Tom1, Vamp1, Tmed2, and Sytl4 are involved in intracellular protein transport. Tom1 is a cytosolic syntaxin-binding protein that negatively regulates synaptic vesicle priming in the intact nervous system[15]. Ctbp2 is a metabolic enzyme regulated transcription factors, which exclusively localizes within the nucleus[19]. Setd7 is a protein lysine methyltransferase that methylates transcription factors[13]. The methylation of proteins affects a series of biological processes. Setd7 is a lysine monomethyltransferase and is responsible for the methyltransferase activity toward various histone and non-histone substrates. Evidence supports that Setd7 promotes the transcription of monocyte chemoattractant protein-1 to mitigate ER stress[20]. Cold stress (4°C, 1 h per day, 20 weeks) induces ER stress and the production of reactive oxygen species (ROS) in animals[21]. Previous study indicated that Setd7 regulates ROS signaling through mitochondria[22]. Acute activation of thermogenesis in brown adipose tissue is associated with increase in mitochondrial ROS levels[23]. Mitochondrial ROS mediates uncoupling protein 1 to regulate thermogenic energy expenditure in brown adipose tissue[16]. In the present study, the activity of Setd7 was significantly decreased whereas its expression remained unaltered in the pituitary of the CE group. Thus, it is possible that inactivation of Setd7 promotes acutely activated thermogenesis mediated by ROS in brown adipose tissue.

In summary, we demonstrate here for the first time that intermittent cold exposure significantly alters the protein expression profile in the hypothalamus and pituitary. Cdc42, Ptprs, and Setd7 proteins were significantly downregulated upon cold exposure and thus might be considered biomarkers of acute thermogenic activation by cold exposure. These proteins are involved in filopodium assembly, peripheral nervous system neuron axonogenesis, positive regulation of pseudopodium assembly, and cell-cell adhesion process in response to cold exposure. Furthermore, these proteins may play an important role in energy metabolism in response to cold exposure. Further studies should be performed to confirm these changes and elucidate the potential interactions between Cdc42, Ptprs, and Setd7 and energy metabolism during cold exposure.

Acknowledgements

This work was supported by the grants of Tianjin Institute of Environmental and Operational Medicine (BWS17J025).

Authors contributions

Yang D F and Gao W N designed the project. Bian X Y and Li X prepared the manuscript. Xu T, Zhang L, Zhang Y Q, and Wu S performed the experiments. Yang R R, Dong W Y, and Guo C J analyzed the data.

Ethical approval

Female SD rats ranging from 8 weeks in age and weighing between 210-230 g each were used for animal studies. The Animal handling and treatment were approved by the Animal Ethical Committee of the Department of Scientific Management of Tianjin Institute of Environmental and Operational Medicine (IACUC of AMMS-04-2020-017).

Conflict of interest

Yang D F is an Editorial Board Member of the journal. The article was subjected to the journal's standard procedures, with peer review handled independently of this member and her research groups. The authors declare no conflict of interests.

References

[1] Wang X, Su M, Qiu Y, *et al.* Metabolic regulatory network alterations in response to acute cold stress and ginsenoside intervention. J Proteome Res, 2007; 6(9): 3449-3455.

[2] Manfredi L H, Zanon N M, Garófalo M A, *et al.* Effect of short-term cold exposure on skeletal muscle protein breakdown in rats. J Appl Physiol, 2013; 115(10): 1496-1505.

[3] Yüksel Ş, Asma D. Effects of extended cold exposure on antioxidant defense system of rat hypothalamic–pituitary–adrenal axis. J Therm Biol, 2006; 31(4): 313-317.

[4] Mulligan J D, Gonzalez A A, Stewart A M, *et al.* Upregulation of AMPK during cold exposure occurs via distinct mechanisms in brown and white adipose tissue of the mouse. J Physiol, 2007; 580(2): 677-684.

[5] Nomura T, Kawano F, Kang M S, *et al.* Effects of long-term cold exposure on contractile muscles of rats. Jpn J Physiol, 2002; 52(1): 85-93.

[6] Park J J, Lee H, Shin M, *et al.* Short-term cold exposure may cause a local decrease of neuropeptide Y in the rat hypothalamus. Mol cells, 2007; 23(1): 88-93.

[7] Labbé S M, Caron A, Lanfray D, *et al.* Hypothalamic control of brown adipose tissue thermogenesis. Front Syst Neurosci, 2015; 9:150.

[8] van der Lans A A, Hoeks J, Brans B, *et al.* Cold acclimation recruits human brown fat and increases nonshivering thermogenesis. J Clin Invest, 2013; 123(8): 3395-3403.

[9] Lee P, Linderman J D, Smith S, *et al.* Irisin and FGF21 are cold-induced endocrine activators of brown fat function in humans. Cell Metab, 2014; 19(2): 302-309.

[10] Rondeel J M, de Greef W J, Hop W C, *et al.* Effect of cold exposure on the hypothalamic release of thyrotropin-releasing hormone and catecholamines. Neuroendocrinology, 1991; 54(5): 477-481.

[11] Brissoni B, Agostini L, Kropf M, *et al.* Intracellular Trafficking of Interleukin-1 Receptor I Requires Tollip. Currt Biol, 2006; 16(22): 2265-2270.

[12] Zhao L J, Subramanian T, Zhou Y, *et al.* Acetylation by p300 regulates nuclear localization and function of the transcriptional corepressor CtBP2. J Biol Chem, 2006; 281(7): 4183-4189.

[13] Cao L, Ren Y, Guo X, *et al.* Downregulation of SETD7 promotes migration and invasion of lung cancer cells via JAK2/STAT3 pathway. Int J Mol Med, 2020; 45(5): 1616-1626.

[14] Ramchandran R, Mehta D, Vogel S M, *et al.* Critical role of Cdc42 in mediating endothelial barrier protection in vivo. Am J Physiol Lung Cell Mol Physiol, 2008; 295(2): L363-369.

[15] Chen Y, Lin J, Chen J, *et al.* Mfn2 is involved in intervertebral disc degeneration through autophagy modulation. Osteoarthritis Cartilage, 2020; 28(3): 363-374.

[16] Davis T B, Yang M, Schell M J, *et al.* PTPRS regulates colorectal cancer RAS pathway activity by inactivating Erk and preventing its nuclear translocation. Sci Reps, 2018; 8(1): 9296.

[17] Heasman S J, Ridley A J. Mammalian Rho GTPases: new insights into their functions from in vivo studies. Nat Rev Mol Cell Biol, 2008; 9(9): 690-701.

[18] Castellani J W, Young A J. Human physiological responses to cold exposure: Acute responses and acclimatization to prolonged exposure. Auton Neurosci, 2016; 196:63-74.

[19] Lei M, Zhang D, Sun Y, *et al.* Web-based transcriptome analysis determines a sixteen-gene signature and associated drugs on hearing loss patients: A bioinformatics approach. J Clin Lab Anal, 2021; 35(12): e24065.

[20] Nobes C D, Hall A. Rho, rac, and cdc42 GTPases regulate the assembly of multimolecular focal complexes associated with actin stress fibers, lamellipodia, and filopodia. Cell, 1995; 81(1): 53-62.

[21] Dai M X, Zheng X H, Yu J, *et al.* The Impact of intermittent and repetitive cold stress exposure on endoplasmic reticulum stress and instability of atherosclerotic plaques. Cell Physiol Biochem, 2014; 34(2): 393-404.

[22] He S, Owen D R, Jelinsky S A, *et al.* Lysine methyltransferase SETD7 (SET7/9) Regulates ROS Signaling through mitochondria and NFE2L2/ARE pathway. Sci Rep, 2015; 5(1): 14368.

[23] Chouchani E T, Kazak L, Jedrychowski M P, *et al.* Mitochondrial ROS regulate thermogenic energy expenditure and sulfenylation of UCP1. Nature, 2016; 532(7597): 112-116.